DOI: 10.61782/fa.2023.0768

forum acusticum 2023

MODELING AND MEASUREMENTS OF THE *F*-HOLE SHAPE'S INFLUENCE ON THE BENDING MODES OF A FRACTIONAL-SIZE VIOLIN

Samuel D. Bellows[1*] **Daisuke Nakayama**[2]
[1] Acoustics Research Group, Department of Physics and Astronomy, Brigham Young University, USA
[2] Yamaha Corporation, Hamamatsu, Japan

ABSTRACT

The violin's f-hole shape plays a significant role in determining the instrument's modal response. Researchers have long studied the influence of the f-hole shape on the A0 or Helmholtz mode through simplified lumped-element representations of this resonator-like mode. Nonetheless, the f-hole shape's impact on the violin's other modes remains ambiguous, partly due to the difficulties of modeling the instrument's coupled acoustic and structural modal response. This work presents a coupled structural-acoustic model to predict how the f-hole shape alters the violin's signature modes. The simulated results suggest that increasing the f-hole aperture size increases the radiated sound power of the B1- structural mode. Sequential measurements on a fractional-size violin using two different f-hole shapes confirm the trend, highlighting the utility of altering the f-hole shape to tune the violin's modal response.

Keywords: *violin, coupled analysis, modal analysis, FEM, BEM.*

1. INTRODUCTION

The violin's f-holes play a critical role in the violin's sound [1]. These stylized cuts into the violin top plate enable an air resonance that functions similarly to a Helmholtz resonator and provides substantial acoustic support for the lowest tones of the violin [2–4]. As the f-holes modify top-plate geometry, they also influence the violin's structural modes [5, 6]. Consequently, understanding the f-hole's acoustic and structural function is of principal concern for luthiers and acousticians.

Researchers have undertaken numerous studies on the acoustics of the violin's f-holes. A series of experiments by Saunders [7] in 1953 suggested that increasing the f-hole length increased the radiated pressure levels not only for the Helmholtz or A0 mode but also at higher frequencies. He inferred that these increased levels at higher frequencies were partly due to stronger vibrations of the bridge island region, the top-plate region between the two f-holes. Because plugging the f-holes with cotton only strongly impacted radiated levels near the A0 mode, he suggested that sound radiation through the f-holes may be limited at higher frequencies. These early results highlight the complex relationship between the f-hole shape and the violin's acoustic and structural modes.

Although structural-acoustic coupling is an essential feature of violin acoustics [4, 8, 9], studying the isolated acoustic and structural systems has provided important insights. One popular approach to studying the rigid-wall acoustic response of the violin is through lumped-element modeling of the A0 mode as a Helmholtz resonator. Itokawa and Kumagi [2], Cremer [10], Schelleng [3], and Shaw [11] all used different variations of equivalent circular and elliptical apertures to estimate the acoustic inertness of the f-hole shape. Once calculated, the f-hole inertness and cavity compliance yield an estimate of the Helmholtz resonance of this mode under a rigid body assumption [2], often within very reasonable agreement with experimentally derived values.

More recently, Nia et al. [12] applied a boundary el-

*Corresponding author: samuel.bellows11@gmail.com.
Copyright: ©2023 Bellows and Nakayama. This is an open-access article distributed under the terms of the Creative Commons Attribution 3.0 Unported License, which permits unrestricted use, distribution, and reproduction in any medium, provided the original author and source are credited.

ement method (BEM) technique to numerically evaluate the conductance (inversely proportional to the inertness [13]) of the f-holes. This improved calculation gave better estimates of A0 frequency, obtaining less than 1% RMSD errors between measured and predicted resonant frequencies for a rigid cavity with f-hole shapes. Application of this model suggested that the violin f-hole shape slowly evolved during the classical Cremonese period to a larger aperture size, leading to an increased A0 frequency and a higher radiated sound power at air resonance. These results demonstrate the strong impact of the f-hole's shape on the violin's sound. Nonetheless, while many of these works modeling A0 as a resonator discussed the elastic effects of the violin cavity in lowering the A0 frequency, they relied on empirical or least-squares fits to account for discrepancies between measured elastic-body and predicted rigid-body results.

In another study, Bissinger [14] used an aluminum violin-shaped cavity dubbed "La Empierre" to remove structural-acoustic coupling. A removable top-plate insert enabled variations to the f-hole's shape, including circular, slot, and traditional f-holes. The results showed A0 frequency increased with increasing f-hole aperture, experimentally validating theoretical assumptions based on resonator theory. He also found that f-hole size and position did not strongly impact the other cavity modes.

Other researchers have studied the impact of the f-holes on the structural modes of the violin. Gough [5] used the finite element method (FEM) to study violin top and back plates, including the impact of arching, shape, plate thickness, and material anisotropy. His results showed that slowly introducing the f-holes into the top plate lowers its resonant frequency. In a later study, a similar FEM model calculated the response of the bridge-island region. However, it did not directly consider how f-hole shape changes could impact structural vibrations in this area [6].

Despite these studies' important insights and results, coupled structural-acoustics models and measurements are best suited to understand the violin's complexities. Weinreich et al. [9] studied air-wood coupling using "Le Gruyére," a violin with 65 plug-able holes in the ribs. Modifying the total aperture area with plugs controlled the air mode frequencies without significantly altering the wood modes. The results revealed 'modal veering,' suggesting a strong coupling between the A0 and the lowest bending modes of the violin. Bissinger et al. [1] used patch near-field acoustical holography and scanning laser Doppler vibrometer (SLDV) scans to identify the contribution of sound radiated through the f-holes and from structural vibrations. They found significant sound radiation from the f-holes, even for the structural modes of the violin, suggesting corpus-induced flow.

Thus, research has verified that the f-holes influence the A0 mode and strongly impact the violin's other modes. Nonetheless, outside of the A0 mode, which may be simply modeled using resonator theory, there remains limited information and understanding on how changes in f-hole shape modify the violin's response. This work studies how f-hole shape changes influence the violin's lowest strongly radiating structural modes. First, a coupled structural-acoustic model provides a straightforward method to study the impact of f-hole shape variations on the radiated sound power of the instrument. The model shows that the shape of the f-hole strongly impacts the $B1^-$ mode, including increasing radiation from the f-holes and the violin body. Experimental measurements on a fractional-size violin validate the results, confirming strengthened structural-mode radiation with increased f-hole aperture area.

2. COUPLED SIMULATION

2.1 Simulation Method

Coupled FEM-BEM simulations are a meaningful method to study violin behavior as they incorporate the critical structural-acoustic coupling of the violin [15]. As suggested by Fig. 1, a Yamaha 3/4 size violin served as the reference geometry for the coupled simulations. The violin CAD model includes the top and back plate, ribs, lining, block, neck, fingerboard, nut, soundpost, and bass bar. The model does not have the bridge, tailpiece, pegs, and strings for more straightforward implementation into simulation software.

Estimating the wood's material properties is essential in reliable numerical simulations [16, 17]. Material property values followed from a fitting procedure similar to that used in Ref. [17]. First, SLDV measurements and analysis identified the lowest structural mode shapes and frequencies of tonewood sample plates used in violin construction. Next, FEM models of the tonewood sample plates served as the basis for numerically estimating plate modal frequencies and allowed density estimation from the measured plate mass. Optimized least-squares fits of the tonewood's orthotropic material properties, including its Young's modulus, shear modulus, and Poisson's ratio, ensured consistency between measured and simulated

Figure 1. CAD model of the 3/4 size violin used in the coupled FEM-BEM simulations.

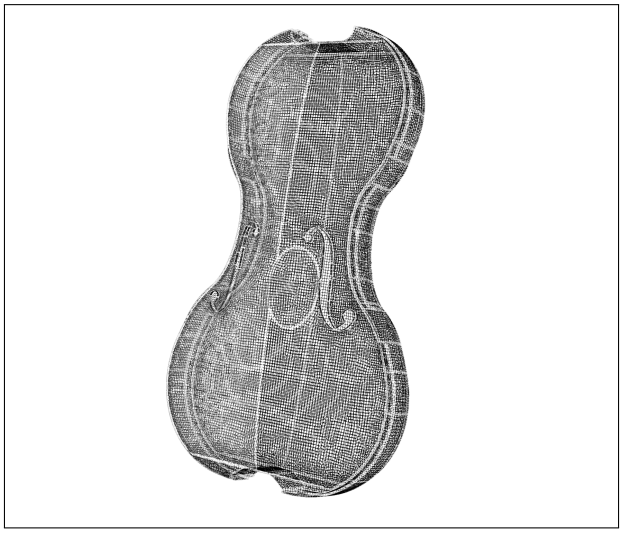

Figure 2. Violin cavity BEM mesh used for the coupled simulations.

modal frequencies.

The simulations used the commercial software ANSYS [18] to estimate the violin's modal frequencies using the FEM without coupling to the acoustic medium. The high-order tetrahedral mesh used for the violin had roughly three million degrees of freedom, comparable to that used by Yokoyama [15]. Free boundary conditions enabled equitable comparisons between later measurements. The analysis identified about 110 structural modes between 0 to 4 kHz.

Figure 2 shows the violin cavity's low-order quadrilateral BEM mesh of around 43,000 elements. This BEM model allows computation of the air resonances of the violin cavity, which are later coupled to the structural modes produced by the FEM model. Additionally, because the violin's top plate, bottom plate, and ribs are very thin (~ 3 mm) relative to the desired wavelengths (> 340 mm), this surface mesh provides a reasonable estimate of the radiated acoustic pressure field provided that radiation from other parts of the violin body, e.g., the neck and fingerboard, are negligible.

An in-house software calculated the coupled FEM-BEM response using a strong coupling technique. A 1 N force applied to a 2 mm square patch near the f-holes served as the excitation force. Six different f-hole scalings based on the same shape allow comparisons between how the f-hole size impacts the radiated response. The smallest pair of f-holes had a total aperture area of 491 mm^2 (70% of the original size), and the largest pair of f-holes had a total apertures area of 1220 mm^2 (110% of the original size). Figure 3 plots these two extremal f-hole pairs on the violin model. Although some size variations are likely too significant for adoption by luthiers, the wide range of f-hole sizes provides essential insight into modal variations due to changes in the overall f-hole aperture.

The present study applied three evaluation surfaces for analysis. The first surface was a 1.5 m radius sphere with 326 nodes centered about the violin. Calculated pressure values on this surface provided estimates of the radiated sound power, directivity, and other radiation properties. The second surface was a rectangular 697-node planar surface placed 1 mm above the apex of the violin top plate. This surface covered the top plate (excluding the fingerboard) to provide a means to study radiation through the f-holes and from the top plate. The third surface was a plane set 15 cm away from the violin top plate; it served as a validation between later measurements made at this same observation distance.

2.2 Sound Power Analysis

The violin's simulated sound power for the six increasing f-hole sizes appears in Fig. 4. Labels indicate the A0, CBR, B1$^-$, and B1$^+$ modes. The sound power results

Figure 3. Smallest (70% of original size) and largest (110% of original size) pair of f-holes on the fractional-size violin model.

show that the A0, B1$^-$, and B1$^+$ modes radiate efficiently while the CBR mode does not, in good agreement with the results from Bissinger et al. [1].

Changes in sound power due to f-hole size reveal several significant trends. First, A0 frequency and radiated sound power increase with enlarged f-hole area, consistent with basic theoretical assertions and previous violin research [12]. Second, although generally considered a structural mode, increasing the f-hole shape significantly impacts the B1$^-$ mode. The sound power curves predict that enlarging the f-hole size will increase B1$^-$ loudness.

The f-hole shape does affect the bending mode B1$^+$, although the impact appears less pronounced than for B1$^-$. Decreasing modal frequency with increasing f-hole size is consistent with the results of Gough, who found that introducing the f-holes into the top plate lowered modal frequencies [5].

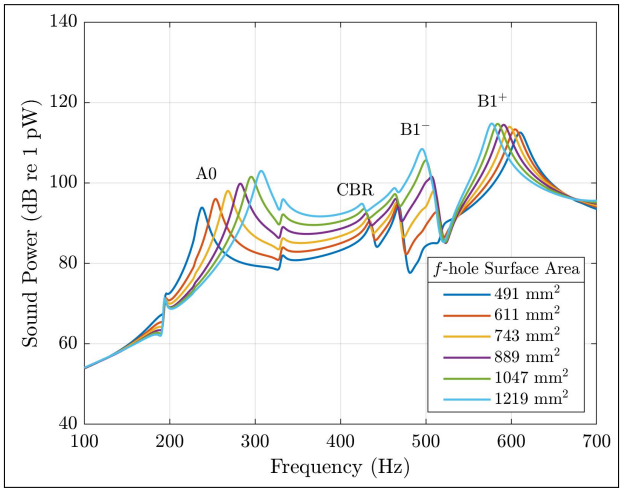

Figure 4. Simulated sound power curves for increasing f-hole size based on a 1 N input force.

2.3 Near-field Analysis

While the sound power curves can reveal how changes in f-hole shape influence radiated levels, they do not provide a complete picture of how the underlying acoustic and structural mechanisms cause these changes. Consequently, near-field analysis provides further insights into variations in acoustic radiation. Figure 5 plots pressure levels of the front evaluation surface calculated at the A0 modal peaks for the six f-hole sizes. The color scale on all plots remains the same to enable equitable comparisons. The white rectangular region in the upper center of the plots corresponds to the area obstructed by the fingerboard.

The surfaces show that increasing f-hole size corresponds to more substantial flow through the f-holes, in agreement with assertions from Nia et al. [12]. The pressure levels around the violin body also suggest that sound radiation for the A0 mode is primarily due to acoustic radiation from the violin cavity through the f-holes rather than structural vibrations, in good agreement with the results of Bissinger et al. [1].

Figure 6 shows the pressure evaluated at the peak of the CBR mode for the six f-hole sizes. The pressure in this plane has strong nulls falling near the center line of the instrument as well as regions of reduced levels. These complex patterns may be associated with CBR's bending motion, which leads to multiple in and out-of-phase regions of corpus vibrations. Unlike for A0, enlarging f-

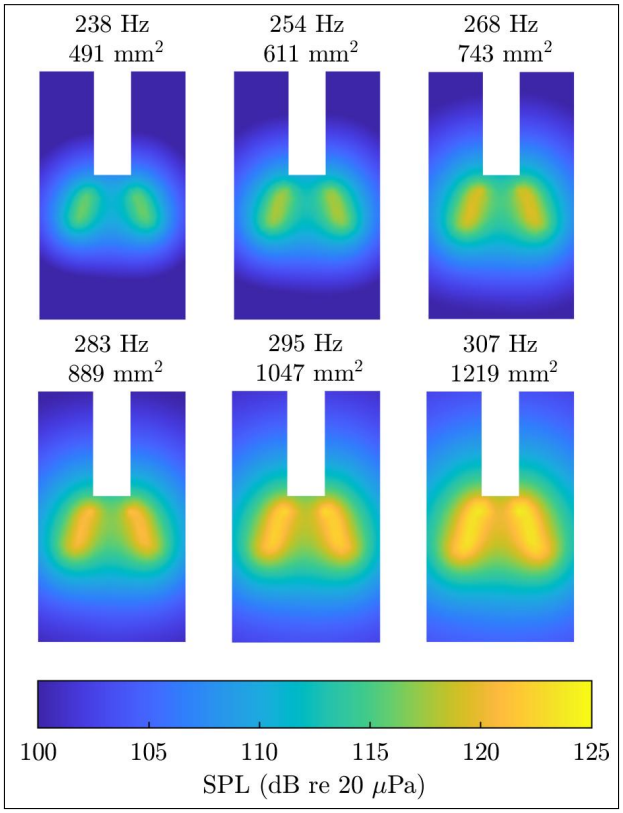

Figure 5. Simulated sound pressure level in the plane directly above the top plate at the A0 resonant peak for the six different f-hole sizes.

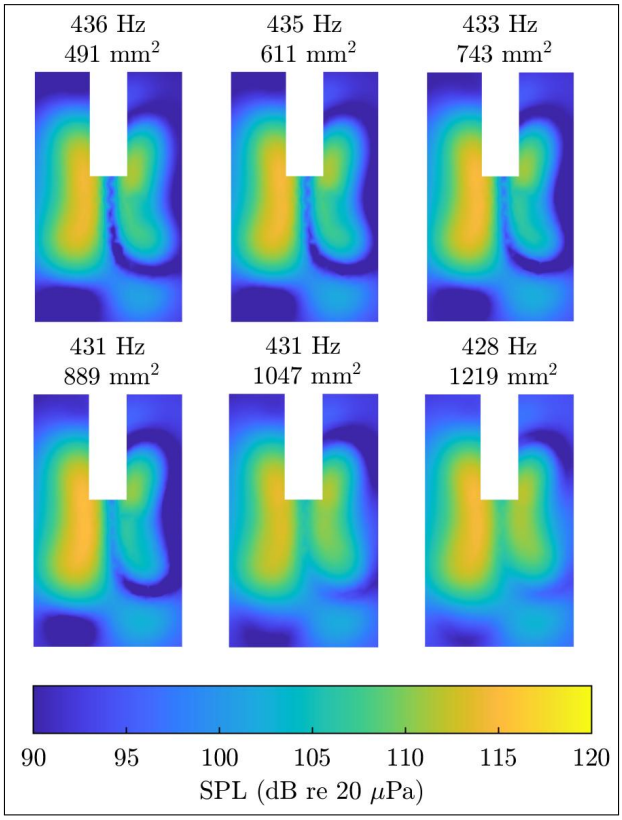

Figure 6. Simulated sound pressure level in the plane directly above the top plate at the CBR resonant peak for the six different f-hole sizes.

hole size appears to have minimal effect on the radiated levels, consistent with the sound power results in Fig. 4.

Figure 7 shows the pressure evaluated at the peak of the $B1^-$ mode for the six f-hole sizes. Similar to the A0 mode, the increased f-hole size corresponds to increased frontal radiation. However, several important trends differ. For the A0 mode, the increased radiation may be directly attributed to increased radiation through the f-holes. However, while increased radiation through the f-holes appears, particularly for the 5th and 6th size variations (500 Hz and 496 Hz), there also is substantial radiation from the bass-bar side lower bout. This result suggests that the increasing sound power for the $B1^-$ mode is due to both increased radiation through the f-holes and stronger vibrations of the violin body.

Figure 8 shows results for the $B1^+$ mode. The changes between f-hole sizes have less effect on the radiated levels, similar to the results seen in the sound power curve of Fig. 4. Consequently, the simulations suggest that f-hole size may be less influential to the $B1^+$ mode compared to A0 and $B1^-$.

3. MEASUREMENTS

While coupled FEM-BEM models can provide some insights into underlying behavior, they are inherently limited due to approximations necessary for practical implementation. Comparisons of radiativity measurements between two different f-holes applied to the same violin help validate observed trends from the simulations. Figure 9 shows the reference 3/4 size Yamaha violin with its original f-hole shape and with an enlarged shape that increased the f-hole's total surface area by around 87% percent. Radiativity tests in an anechoic environment (f_c = 80 Hz) evaluated the acoustic response before and after the f-hole shape change. A force hammer tapped the G-string side

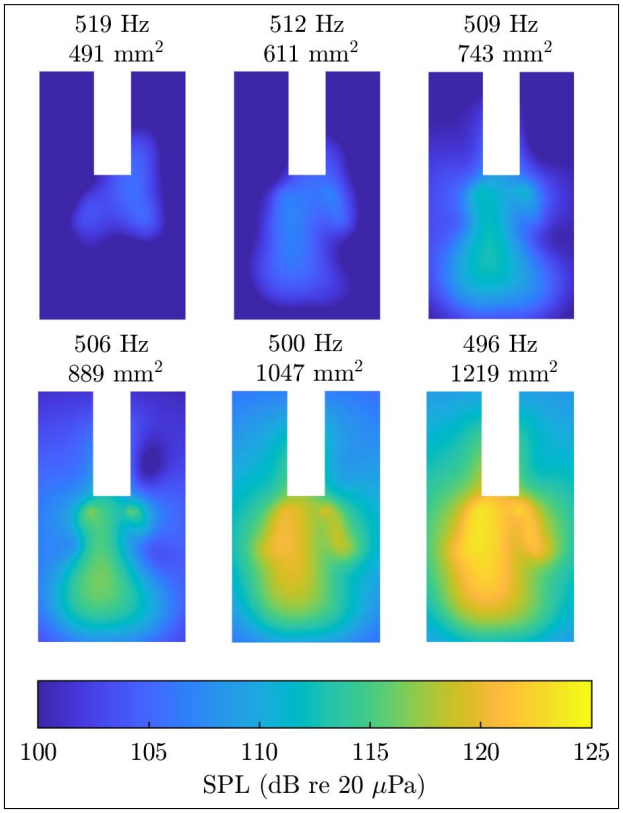

Figure 7. Simulated sound pressure level in the plane directly above the top plate at the $B1^-$ resonant peak for the six different f-hole sizes.

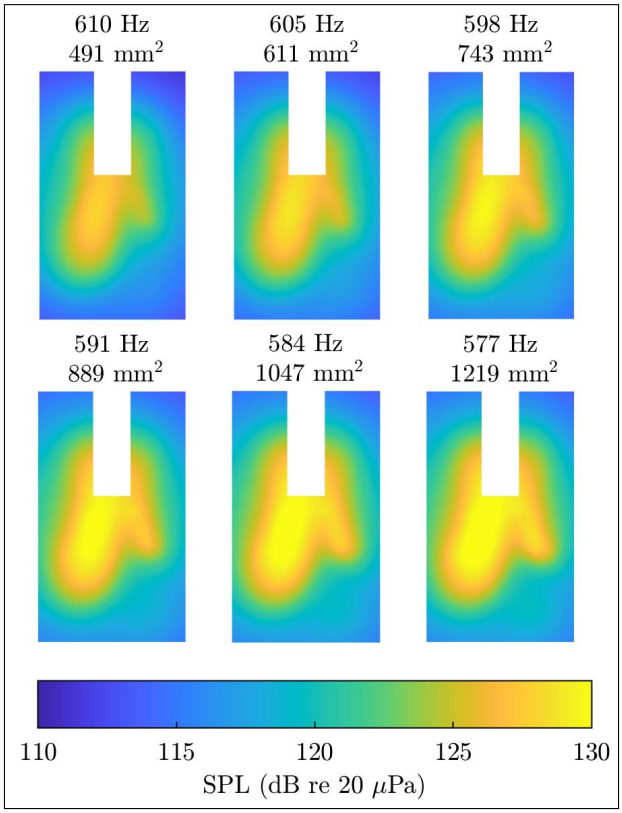

Figure 8. Simulated sound pressure level in the plane directly above the top plate at the $B1^+$ resonant peak for the six different f-hole sizes.

of the bridge, and a 12.7 mm (0.5 in) microphone placed 15 cm from the center of the bridge measured the acoustic output. Elastic strings supported the violin at the neck and scroll to approximately realize free boundary conditions. Figure 10 shows the measurement setup.

Figure 11 compares the measurement results between the coupled model and the measured violin with the original f-hole shape. Similar to the measurement results, the coupled model results followed by evaluating the pressure 15 cm from the center of the bridge based on a 1 N excitation force. Table 1 reports the predicted and measured modal frequencies. For the A0 mode, there is excellent agreement between measurement and simulation for both the radiated levels and A0 resonant frequency. The simulation and measurement frequencies agree well for the CBR, $B1^-$ and $B1^+$, achieving deviations less than 50 cents. However, the accuracy of the predicted peak levels is not as precise as for the A0 mode. While the A0 levels relate to acoustic radiation through the f-holes, radiation from the structural modes strongly depends on the excitation point. The lack of a bridge in the simulation model may explain these level deviations for the violin's structural modes. Additionally, the material properties for the simulation followed from tonewood samples rather than from the violin's body.

Figure 12 plots the measured pressure level for both f-hole shapes as a function of frequency. Several trends predicted by the simulation appear in the measurement results. First, the enlarged f-hole shape significantly alters the A0 mode, increasing both its resonant peak and maximum radiated level. Second, the enlarged f-hole shape slightly lowered both the $B1^-$ and $B1^+$ modal frequencies. Additionally, the enlarged f-hole shape increased the radiated level of the $B1^-$ peak and the radiated levels between A0 and $B1^-$.

While the $B1^+$ mode followed the anticipated trend

Figure 9. Comparison of the violin with its original f-hole shape and after the f-hole enlargement.

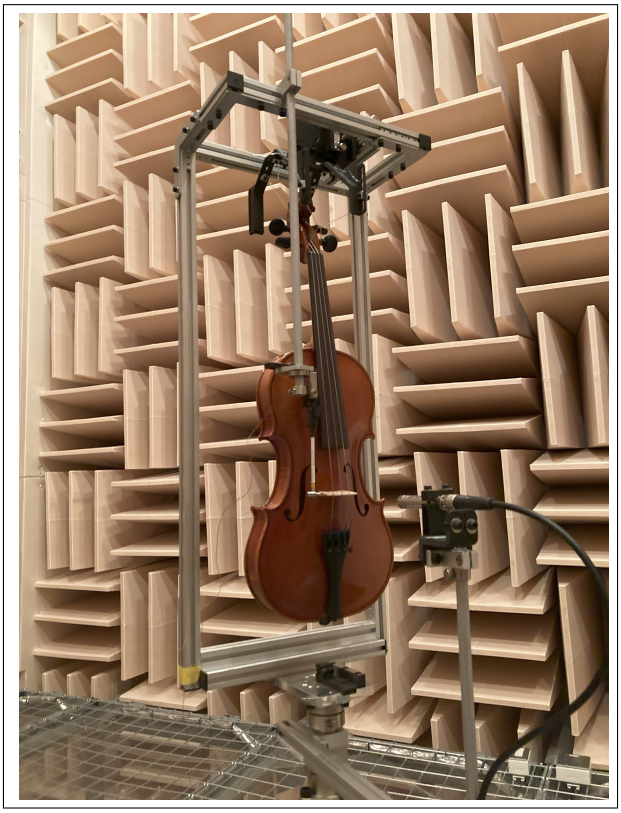

Figure 10. Violin radiativity measurement set-up.

Table 1. Simulated and measured violin modal frequencies.

Mode	Simulated (Hz)	Measured (Hz)	Deviation (Cents)
A0	291	292	6
CBR	424	425	4
$B1^-$	477	483	22
$B1^+$	571	558	40

of a lower modal frequency with a larger f-hole size, the radiated level decreased contrary to expectations. However, several differences between measurements and the simulation's results could impact these deviations. For example, because the enlarged f-hole shape required cutting away material around the f-hole, it was not feasible to maintain the same f-hole shape as done in the simulations. Nonetheless, the general agreement between measurement and simulation highlights the utility of numerical methods in studying violin acoustics.

4. CONCLUSIONS

The f-holes influence the modal characteristics of the violin, both for the A0 air-resonance mode and its structural modes. Through simulations and measurements, this study considered how changes in f-hole size impact the violin's overall acoustic response. The simulations and measurements both confirm that enlarging f-hole size increased A0 frequency and loudness. The results also suggest that enlarged f-hole size increases radiated $B1^-$ levels. Future research includes further studies into full-sized violins and the influence of the f-hole shape on the violin's other signature modes.

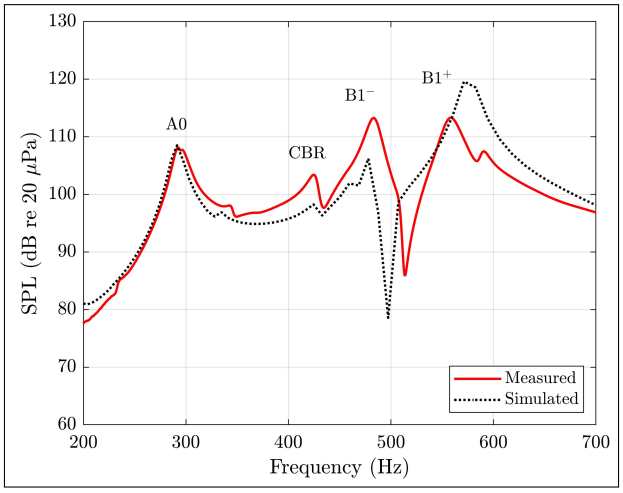

Figure 11. Radiativity curves for the simulated and measured violin.

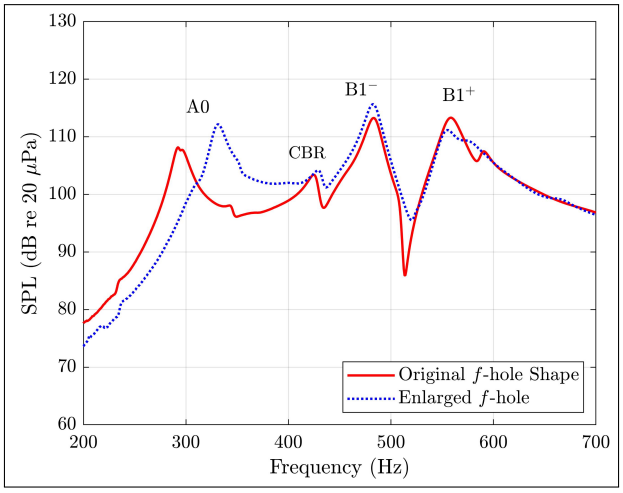

Figure 12. Measured radiativity curves between original and enlarged f-hole shape.

5. REFERENCES

[1] G. Bissinger, E. G. Williams, and N. Valdivia, "Violin f-hole contribution to far-field radiation via patch near-field acoustical holography," *J. Acoust. Soc. Am.*, vol. 121, no. 6, pp. 3899–3906, 2007.

[2] H. Itokawa and C. Kumagai, "Research on violin making," *Inst. Sci. U Tokyo*, vol. 3, pp. 5–19, 1952.

[3] J. C. Schelleng, "The violin as a circuit," *J. Acoust. Soc. Am.*, vol. 35, no. 3, pp. 326–338, 1963.

[4] K. D. Marshall, "Modal analysis of a violin," *J. Acoust. Soc. Am.*, vol. 77, no. 2, pp. 695–709, 1985.

[5] C. Gough, "Violin plate modes," *J. Acoust. Soc. Am.*, vol. 137, no. 1, pp. 139–153, 2015.

[6] C. Gough, "The violin bridge-island input filter," *J. Acoust. Soc. Am.*, vol. 143, no. 1, pp. 1–12, 2018.

[7] F. A. Saunders, "Recent work on violins," *J. Acoust. Soc. Am.*, vol. 25, no. 3, pp. 491–498, 1953.

[8] A. Isaksson, H. O. Saldner, and N.-E. Molin, "Influence of enclosed air on vibration modes of a shell structure," *J. Sound Vib.*, vol. 187, no. 3, pp. 451–466, 1995.

[9] G. Weinreich, C. Holmes, and M. Mellody, "Air-wood coupling and the swiss-cheese violin," *J. Acoust. Soc. Am.*, vol. 108, no. 5, pp. 2389–2402, 2000.

[10] L. Cremer, *The Physics of the Violin*. MIT Press, 1984.

[11] E. A. G. Shaw, "Cavity resonance in the violin: Network representation and the effect of damped and undamped rib holes," *J. Acoust. Soc. Am.*, vol. 87, no. 1, pp. 398–410, 1990.

[12] H. T. Nia, A. D. Jain, Y. Liu, M.-R. Alam, R. Barnas, and N. C. Makris, "The evolution of air resonance power efficiency in the violin and its ancestors," in *Proc. R. Soc. A*, vol. 471, 2015.

[13] A. D. Pierce, *Acoustics*. Springer International Publishing, 2019.

[14] G. Bissinger, "Effect of f-hole shape, area, and position on violin cavity modes below 2 khz," *Catgut Acoust. Soc. J.*, vol. 2 (Ser. II), pp. 12–17, 1992.

[15] M. Yokoyama, "Coupled numerical simulations of the structure and acoustics of a violin body," *J. Acoust. Soc. Am.*, vol. 150, no. 3, pp. 2058–2064, 2021.

[16] A. Brauchler, P. Ziegler, and P. Eberhard, "An entirely reverse-engineered finite element model of a classical guitar in comparison with experimental data," *J. Acoust. Soc. Am.*, vol. 149, no. 6, pp. 4450–4462, 2021.

[17] H. Tahvanainen, H. Matsuda, and R. Shinoda, "Numerical simulation of the acoustic guitar for virtual prototyping," in *Proceedings of ISMA 2019*, pp. 13–17, 2019.

[18] *Ansys Mechanical*. ANSYS Inc., 2022.